IEICE TRANS. COMMUN., VOL.E94–B, NO.5 MAY 2011

LETTER *Special Section on Antenna and Propagation Technologies Contributing to Diversification of Wireless Technologies*

Channel Capacity Improvement in Short-Range MIMO Using Side and Back Reflectors

Hiroshi HIRAYAMA[†a)], ***Member***, **Gen MATSUI**[†], ***Student Member***, **Nobuyoshi KIKUMA**[†], ***and*** **Kunio SAKAKIBARA**[†], ***Members***

SUMMARY A new structure to improve channel capacity of short-range MIMO is proposed. The proposed structure consists of back reflector and side reflector. FDTD simulation demonstrates a role of back reflector and side reflector. The back reflector increases all eigen values. The side reflector equalizes eigen value distribution. Consequently, the proposed structure enhances the channel capacity.

key words: *short-range MIMO, FDTD, eigen value distribution, MIMO antenna*

1. Introduction

The conventional MIMO systems have a capability of enhancing channel capacity by exploiting multipath environment [1]. Recently, a novel scheme of MIMO system for short-range communication has proposed [2]. In the short-range MIMO system, channel capacity is able to be improved without a multipath, because spherical wave is considered as a superposition of plane waves. It is expected that the short-range MIMO system enables us to realize high-speed short-range wireless communications.

In this report, we propose a new antenna structure using back reflector and side reflector to improve channel capacity for short-range MIMO.

2. Basic Characteristics of the Short-Range MIMO

2.1 Calculation Model

To maximize channel capacity in eigen-mode transfer, equalizing eigen values of $\mathbf{H}^H\mathbf{H}$ is required, where $\mathbf{H}$ is a channel response matrix and $()^H$ shows conjugate transpose. To achieve this goal, understanding propagation mechanism of the eigen mode is useful. At first, we investigate basic characteristics of short-range MIMO with FDTD simulation. In the conventional MIMO, ray-tracing techniques are often used to calculate channel response matrix.

Although ray-tracing techniques assume plane wave propagation, it has a capability of taking account of spherical wave fronts [3]. An advantage of using FDTD is that the full-wave technique has a capability of including all electromagnetics: mutual effect between TX element and RX element or effect of reflectors.

Manuscript received September 2, 2010.
Manuscript revised December 17, 2010.

[†]The authors are with the Dept. of Computer Science, Nagoya Institute of Technology, Nagoya-shi, 466-8555 Japan.
a) E-mail: hirayama@nitech.ac.jp

DOI: 10.1587/transcom.E94.B.1280

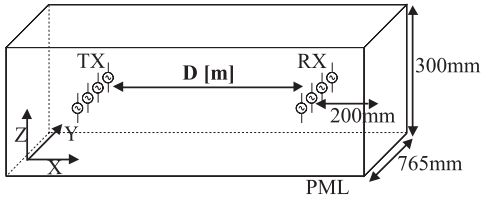

Fig. 1 Configuration of the TX and RX antennas and the calculation region for FDTD simulation.

Table 1 Eigenvalues.

Eigen mode	FDTD [dB]	Theoretical [dB]
1st	0	0
2nd	−14.5	−14.1
3rd	−37.6	−37.9
4th	−54.3	−70.3

Figure 1 shows a calculation model of the FDTD simulation. Four half-wavelength dipole antennas are used for TX and RX. Element spacing is set to 55 mm. Distance between TX and RX antennas (D) is 1 m. Perfect matched layer (PML) is used as absorption boundary condition. One of the TX element is excited at 2.45 GHz. Another TX elements and RX elements are terminated with 50 Ω. FDTD simulation is repeated four times by alternating antenna element to excite. Channel response matrix $\mathbf{H} = [h_{ki}]$ is obtained from the complex voltage h_{ki} of the k-th RX element when the i-th TX element is excited.

2.2 Consideration

Eigen values of the $\mathbf{H}^H\mathbf{H}$, which equal to the power of the singular values of $\mathbf{H}$, are shown Table 1. Theoretical values obtained from geometrical optics approximation are also shown in Table 1. The FDTD and the theoretical values for the 1st, 2nd, and 3rd eigen values are similar. However, they are different for the 4th eigen value. It is considered that the 4th eigen value includes effect of mutual coupling between the elements and calculation error of the FDTD simulation caused by reflection from the PML and discretization error.

In the conventional MIMO, eigen beam pattern is used to evaluate eigen beam. Let $\mathbf{e}_t^n$ and $\mathbf{e}_r^n$ be a weight vector of TX and RX for the n-th eigen mode, respectively. $\mathbf{e}_t^n$ and $\mathbf{e}_r^n$ are calculated by singular value decomposition (SVD) of the channel response matrix $\mathbf{H}$:

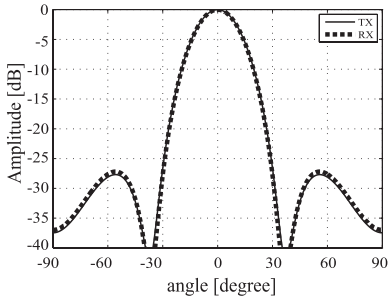

(a) The 1st eigen mode

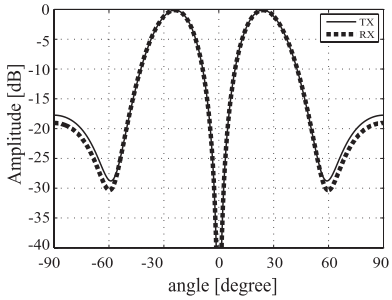

(b) The 2nd eigen mode

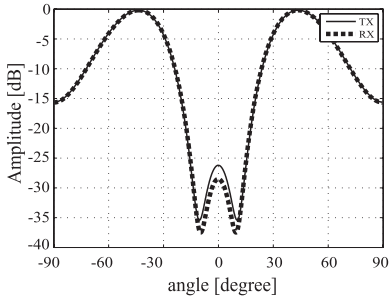

(c) The 3rd eigen mode

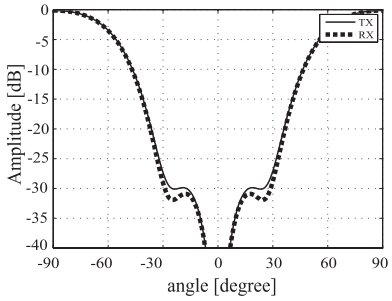

(d) The 4th eigen mode

Fig. 2 Far-field patterns of the eigen modes.

$$\mathbf{H} = \mathbf{E}_r \mathbf{D} \mathbf{E}_t^H \tag{1}$$

where

$$\mathbf{E}_t = \left[\mathbf{e}_t^1, \cdots, \mathbf{e}_t^N\right] \tag{2}$$

$$\mathbf{E}_r = \left[\mathbf{e}_r^1, \cdots, \mathbf{e}_r^N\right] \tag{3}$$

$$\mathbf{D} = \mathrm{diag}\left(\sqrt{\lambda_1}, \cdots, \sqrt{\lambda_N}\right) \tag{4}$$

and λ_n is an eigen value of $\mathbf{H}^H\mathbf{H}$. N is a number of antennas. The eigen beam pattern of TX and RX is calculated as an array factor whose weight is $\mathbf{e}_t^n$ and $\mathbf{e}_r^n$, respectively. Figure 2 shows eigen beam patterns of the TX and the RX obtained from the FDTD simulation. Phase of the TX weight is listed in Table 2. In this configuration, the RX antenna is located at 0 degree direction from the TX antenna. According to the 1st eigen mode, all TX elements are excited in-phase, then the eigen beam directs 0 degree direction. However, although the 2nd eigen value is −14.5 dB, deep null is formed for 0 degree direction in the 2nd eigen beam. This inconsistency is caused by applying far-field pattern to the near-field region. Therefore, in the short-range MIMO, eigen beam pattern is not adequate to evaluate eigen mode.

Table 2 Phase of TX weight for eigen modes.

Eigen mode	Phase of antenna elements			
	1st [deg]	2nd [deg]	3rd [deg]	4th [deg]
1st	+147.1	+161.3	+161.3	+147.1
2nd	+28.8	+44.2	−135.7	−151.1
3rd	+42.5	−151.7	−151.7	+42.5
4th	+91.3	−104.1	+75.9	−88.7

Instead of the eigen beam pattern, electric field distribution of eigen mode is conducted to consider eigen mode. Electric Field distribution of n-th eigen mode $E^n(x, y, z)$ is calculated by

$$E^n(x, y, z) = \sum_{i=1}^{N} w_i^n E_i(x, y, z), \tag{5}$$

where w_i^n is the i-th component of the singular vector of n-th singular value, and $E_i(x, y, z)$ is z-component of an electric field distribution when the i-th TX element is excited. Figure 3 shows the calculation result. We can understand that an azimuth angle of the eigen beam increases in accordance with increase of index of eigen modes to form eigen modes on the RX antennas. Consequently the 2nd, 3rd, and 4th eigen value decreases.

3. Improvement of Short-Range MIMO

3.1 Proposed Structure

In order to improve channel capacity in MIMO system, not only enlarging signal to noise ratio (SNR) but also equalizing eigen values of channel matrix is important. Figure 4 shows proposed structure for short-range MIMO. This structure consists of half-wavelength dipole antennas, back reflector, and side reflectors. The back reflector is located quarter-wavelength behind the antennas, thus the beam directs broadside direction. The side reflectors whose length is d are located both endfire direction.

3.2 Effect of the Reflectors

Using this structure both for TX and RX antenna, FDTD simulation is performed.

Figure 5 shows eigen value distributions as a function of distance between the TX and RX antenna. The dot line

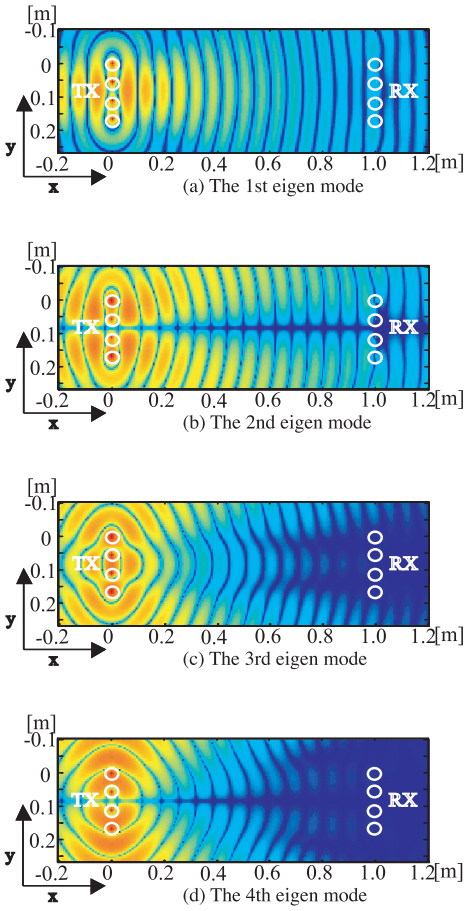

Fig. 3 Electric-field distributions of the eigen modes.

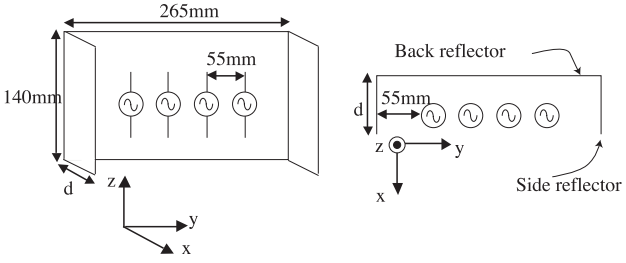

Fig. 4 Proposed structure of antenna for short-range MIMO system.

is for the case of without the back reflector nor the side reflector, the dashed line is for only with the back reflector without the side reflector, and the solid line is for the case with the back reflector and the side reflector.

In comparison of the dot line and the dashed line in Fig. 5, back reflector increases all eigen values equally. In comparison of the solid line and the dashed line in Fig. 5, side reflector increases the 2nd, 3rd, and 4th eigen values.

Channel capacity is calculated from these eigen values.

Assuming the water-filling theorem, channel capacity for MIMO C_{MIMO} is calculated by

$$C_{MIMO} = \sum_{i=1}^{N} \log_2 (1 + \lambda_i \gamma_i), \tag{6}$$

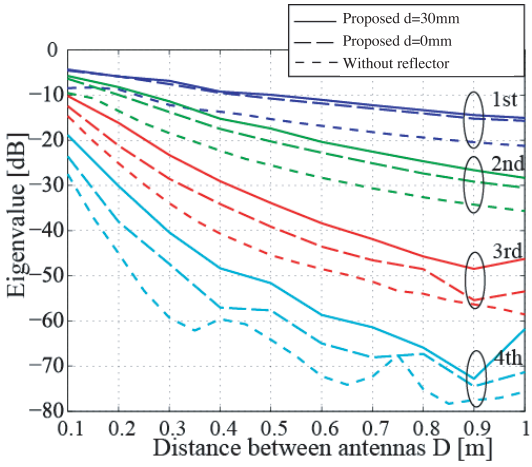

Fig. 5 Dependency of the distance between TX and RX antennas on the eigen values.

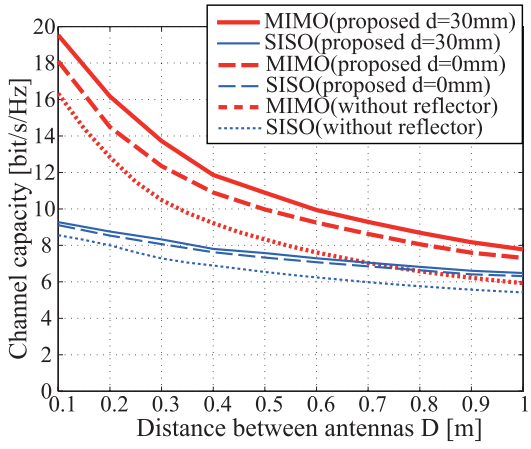

Fig. 6 Dependency of the distance between TX and RX antennas on the channel capacity.

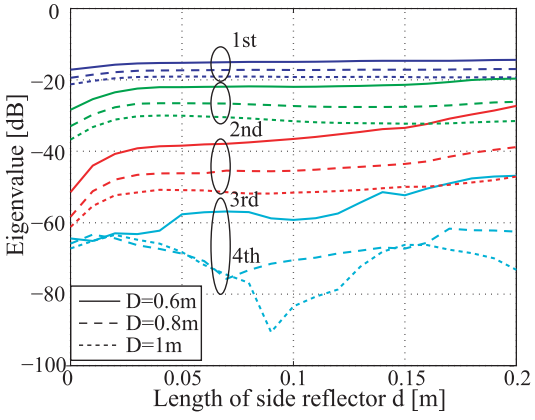

Fig. 7 Dependency of the length of the side reflector on the eigen values.

where γ_i is SNR, which is calculated to fulfill

$$\sum_{i=1}^{N} \gamma_i = \gamma_0 \tag{7}$$

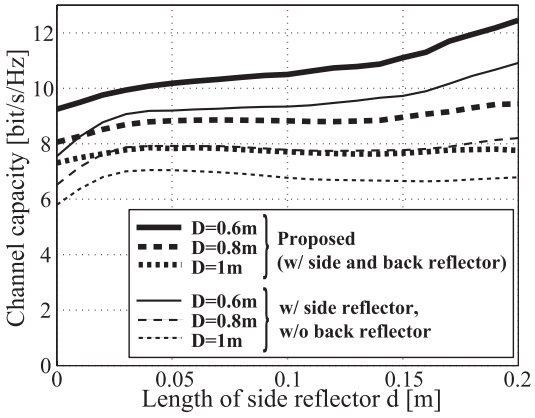

Fig. 8 Dependency of the length of the side reflector on the channel capacity.

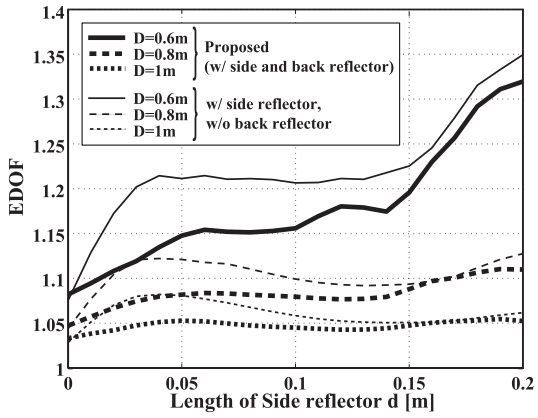

Fig. 9 Dependency of the length of the side reflector on the EDOF.

with the water-filling theorem [4]. γ_0 is obtained by assuming that TX power is 0 dBm and noise power in RX of each channel is −100 dBm. Channel capacity for SISO transfer C_{SISO} is also calculated by

$$C_{SISO} = \log_2(1 + \gamma_0). \tag{8}$$

In this case, received power of four antennas are added and used as a signal power for the calculation of γ_0.

Figure 6 shows the calculation result. Using of the back reflector increases channel capacity both for SISO and MIMO. On the other hands, using of the side reflector increases channel capacity only for MIMO.

From this result, a role of side reflector is to equalize eigenvalue distribution.

3.3 Effect of the Length of Side Reflectors

To understand an effect of length of side reflector, eigen value distributions as a function of a length of side reflector is shown in Fig. 7. The 1st eigen value does not vary by changing the length of side reflector. On the other hands, the 2nd and the 3rd eigen values are increased in accordance with extending side reflector. Therefore, it is said that the side reflector has affect to equalize eigen value distribution. Considering the electric field distribution of 2nd, 3rd, and 4th eigen mode shown in Fig. 3, it is said that the oblique incident wave is reflected by the side reflector, then those eigen values were increased.

Channel capacity is shown in Fig. 8. To distinguish the effect of the back reflector and the side reflector, channel capacity only with the side reflector, without the back reflector is also plotted. For both cases, extending side reflector enlarges channel capacity.

As an index of equality of eigen value distribution, effective degrees of freedom (EDOF) is conducted [5]. The EDOF is defined by

$$EDOF = \frac{\sum_{i=1}^{N} \lambda_i}{\lambda_1}. \tag{9}$$

In the worst case, such as pin-hole model propagation, EDOF becomes 1, and in the best case, EDOF becomes the number of antennas. Calculated EDOF is shown in Fig. 9. The improvement of EDOF by extracting the length of the side reflector is more effective when the distance between TX and RX is closed.

In comparison of the thick line and the thin line in Fig. 9, use of back reflector decreases the EDOF. It is considered that the back reflector increases spatial correlation since the back reflector increases mutual coupling between elements. However, because of the effect of increasing all eigen values, channel capacity is increased.

4. Conclusion

We proposed an antenna structure to improve channel capacity of short-range MIMO. FDTD simulation demonstrates a role of back reflector and side reflector.

The back reflector increases all eigen values. The side reflector equalizes eigen value distribution. Consequently, the proposed structure enhances the channel capacity.

To find optimum parameters of the structure is further study.

References

[1] Y. Karasawa, "Innovative antennas and propagation studies for MIMO systems," IEICE Trans. Commun., vol.E90-B, no.9, pp.2194–2202, Sept. 2007.
[2] N. Honma, K. Nishimori, T. Seki, and M. Mizoguchi, "Short range MIMO communication," Proc. EuCAP 2009, pp.1763–1767, March 2009.
[3] J.S. Jiang and M.A. Ingram, "Spherical-wave model for short-range MIMO," IEEE Trans. Antennas Propag., vol.53, no.9, pp.1534–1541, Sept. 2005.
[4] Y. Karasawa, "MIMO propagation channel modeling," IEICE Trans. Commun., vol.E88-B, no.5, pp.1829–1842, May 2003.
[5] J.W. Wallace and M.A. Jensen, "MIMO capacity variation with SNR and multipath richness from full-wave indoor FDTD simulations," Proc. APS 2003, vol.2, pp.523–526, June 2003.